Programmable digital memory devices based on nanoscale thin films of a thermally dimensionally stable polyimide

2009 Nanotechnology 20 135204

(http://iopscience.iop.org/0957-4484/20/13/135204)

Nanotechnology **20** (2009) 135204 (7pp) doi:10.1088/0957-4484/20/13/135204

Programmable digital memory devices based on nanoscale thin films of a thermally dimensionally stable polyimide

Taek Joon Lee[1,4], Cha-Wen Chang[2,4], Suk Gyu Hahm[1], Kyungtae Kim[1], Samdae Park[1], Dong Min Kim[1], Jinchul Kim[1], Won-Sang Kwon[1], Guey-Sheng Liou[3,5] and Moonhor Ree[1,5]

[1] Department of Chemistry, National Research Lab for Polymer Synthesis and Physics, Center for Integrated Molecular Systems, Polymer Research Institute, and BK School of Molecular Science, Pohang University of Science and Technology, Pohang 790-784, Republic of Korea
[2] Department of Applied Chemistry, National Chi Nan University, 1 University Road, Puli, Nantou Hsien 54561, Taiwan, Republic of China
[3] Institute of Polymer Science and Engineering, National Taiwan University, Taipei 10617, Taiwan, Republic of China

E-mail: gsliou@ntu.edu.tw and ree@postech.edu

Received 13 November 2008
Published 10 March 2009
Online at stacks.iop.org/Nano/20/135204

Abstract

We have fabricated electrically programmable memory devices with thermally and dimensionally stable poly(N-(N',N'-diphenyl-N'-1,4-phenyl)-N,N-4,4′-diphenylene hexafluoroisopropylidene-diphthalimide) (6F-2TPA PI) films and investigated their switching characteristics and reliability. 6F-2TPA PI films were found to reveal a conductivity of 1.0×10^{-13}–1.0×10^{-14} S cm^{-1}. The 6F-2TPA PI films exhibit versatile memory characteristics that depend on the film thickness. All the PI films are initially present in the OFF state. The PI films with a thickness of >15 to <100 nm exhibit excellent write-once-read-many-times (WORM) (i.e. fuse-type) memory characteristics with and without polarity depending on the thickness. The WORM memory devices are electrically stable, even in air ambient, for a very long time. The devices' ON/OFF current ratio is high, up to 10^{10}. Therefore, these WORM memory devices can provide an efficient, low-cost means of permanent data storage. On the other hand, the 100 nm thick PI films exhibit excellent dynamic random access memory (DRAM) characteristics with polarity. The ON/OFF current ratio of the DRAM devices is as high as 10^{11}. The observed electrical switching behaviors were found to be governed by trap-limited space-charge-limited conduction and local filament formation and further dependent on the differences between the highest occupied molecular orbital and the lowest unoccupied molecular orbital energy levels of the PI film and the work functions of the top and bottom electrodes as well as the PI film thickness. In summary, the excellent memory properties of 6F-2TPA PI make it a promising candidate material for the low-cost mass production of high density and very stable digital nonvolatile WORM and volatile DRAM memory devices.

(Some figures in this article are in colour only in the electronic version)

1. Introduction

Electrically bistable resistive switching organic and polymeric materials have significant advantages over inorganic silicon- and metal-oxide-based memory materials in that their dimensions can easily be miniaturized and their properties can easily be tailored during chemical synthesis [1–15]. In recent years, the use of organic and polymeric materials in memory devices has indeed attracted significant attention [1–15]. However, organic materials are susceptible to damage during the

[4] T J Lee and C-W Chang contributed equally to this work.
[5] Authors to whom any correspondence should be addressed.

processing involved in the fabrication of memory devices because of their low boiling points and low chemical resistance, and they also require more elaborate and expensive processing such as vacuum evaporation and deposition [1–4].

In contrast, polymer materials exhibit easy processability, flexibility, high mechanical strength and good scalability. Further, they can be processed at low cost, and with their use the three-dimensional (3D) multi-stack layer structures required for high density memory devices can easily be fabricated. As a result, significant research effort is currently being invested in the development of polymer switching materials with properties and processability that meet the requirements of memory devices. Several studies have reported such polymer materials [5–15]. However, most of these polymers have aliphatic hydrocarbon backbones that exhibit low-dimensional stability [5–8], high ON and OFF switching voltages [7, 8] and high OFF currents [7, 8]. Thus the development of highly stable memory devices based on dimensionally and thermally stable polymers remains in the exploration stage.

Aromatic polyimides (PIs) have been well known to have excellent thermal stability, dimensional stability, mechanical properties, optical transparency, adhesion and chemical resistance [16–18]. Furthermore, they can be easily fabricated as films by conventional, simple spin-, bar-, roll-or dip-coating processing of their solutions in organic solvents [16–18]. Because of the advantageous properties and excellent processability, aromatic PIs are widely used as interdielectric layers and flexible carriers in microelectronic devices [16] and liquid crystal (LC) alignment layers in LC flat-panel display devices [17, 18].

In this study, we report the fabrication of high performance programmable memory devices based on thin films of a thermally dimensionally stable polyimide (PI), poly(*N*-(*N*′,*N*′-diphenyl-*N*′-1,4-phenyl)-*N*,*N*-4,4′-diphenylene hexafluoroisopropylidene-diphthalimide) (6F-2TPA PI) (figure 1). This PI is easily processed with conventional solution spin-, roll- or dip-coating and subsequent drying. The electrodes in the devices were prepared by evaporation. These devices exhibit excellent write-once-read-many-times memory (WORM) and dynamic random access memory (DRAM) characteristics with a high ON/OFF ratio, and can be fabricated in three-dimensional arrays that provide very high density storage. Furthermore, the 6F-2TPA PI has high thermal and dimensional stability and can thus be hybridized with a complementary metal-oxide-semiconductor platform.

2. Experimental details

6F-2TPA PI was prepared from 2,2′-bis-(3,4-dicarboxyphenyl) hexafluoropropane dianhydride (6F) and *N*-(*N*′,*N*′-diphenyl-*N*′-1,4-phenyl)-*N*, *N*-4,4′-diphenylene diamine (2TPA) according to a previously reported synthetic method [19]. For the fabrication of memory devices, homogeneous 6F-2TPA solutions (0.5–4.0 wt%) were prepared in cyclopentanone and then filtered using polytetrafluoroethylene-membrane-based (PTFE) microfilters with a pore size of 0.45 μm. Single-active-layer memory devices were then fabricated as follows.

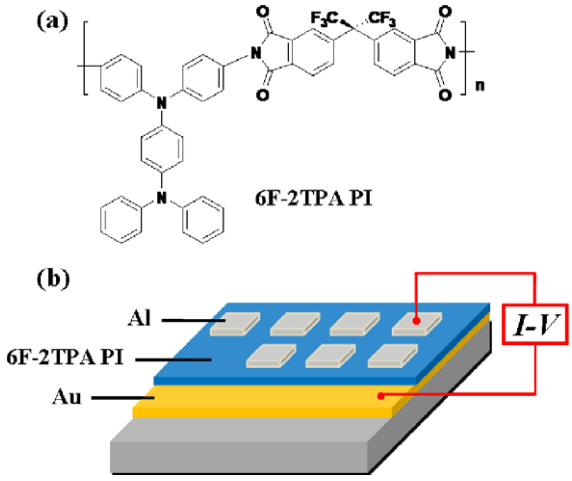

Figure 1. (a) Chemical structure of 6F-2TPA PI and (b) a schematic diagram of the memory devices fabricated in this study.

The polymer solutions were spun onto precleaned silicon wafers deposited with an Au or Al layer (with a thickness of 300 nm) by electron-beam sputtering; a spin-coating process of 2000 rpm/40 s was employed. The spun films were dried in vacuum on a hot plate at 80 °C for 5 h. The thicknesses of the resulting films were determined using a spectroscopic ellipsometer (model VASE, Woollam). The Al and Au electrodes were deposited onto the polymer films (coated on the substrates) at a pressure below 10^{-7} Torr by means of thermal evaporation. The top metal electrodes were determined to have a thickness of 300 nm, with sizes between 0.5 × 0.5 mm^2 and 2.0 × 2.0 mm^2. All electrical experiments were conducted in air ambient, without any device encapsulation. The *I*–*V* measurements and electrical-stress tests were carried out with forward and reverse voltage scans between −4.0 V (or −8.0 V) and +4.0 V (or +8.0 V) at a scan rate of 500 mV s^{-1} using a Keithley 4200-SCS semiconductor parameter analyzer. In addition, the electrical DC conductivities of the films were measured using a four-point probe or a two-point probe connected to the Keithley semiconductor parameter analyzer. Surface roughness and morphology were examined with an atomic force microscope (Multimode AFM Nanoscope IIIa, Digital Instruments).

3. Results and discussion

The 6F-2TPA PI (figure 1(a)) was found to be thermally stable up to 550 °C in air and nitrogen atmospheres. 6F-2TPA PI films were coated onto gold (Au) and aluminum (Al) substrates and examined with atomic force microscopy (AFM), and found to have root-mean-square (rms) surface roughnesses of 1.56 nm on Au and 2.43 nm on Al over an area of 1.0 × 1.0 μm^2 (data not shown). These values show that the bottom electrodes have smooth surfaces. We also examined 74 nm thick 6F-2TPA PI films coated onto Au and Al electrodes with AFM. The AFM analysis confirmed that simple and conventional spin-coating of the 6F-2TPA PI yields excellent quality nanoscale thin films. The rms roughness values of the PI thin film surfaces were found to be 0.34 nm for the Au electrode and 0.31 nm for the Al

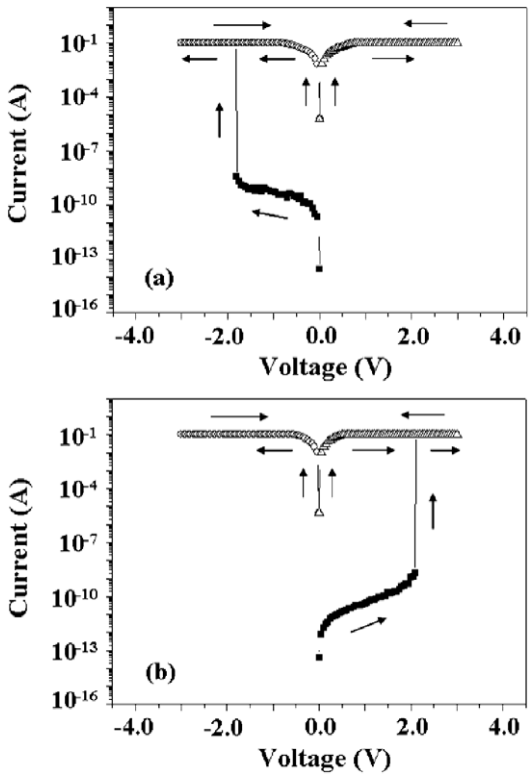

Figure 2. I–V curves for the Au/6F-2TPA PI (74 nm thick)/Al device: (a) the applied voltage was swept from 0 to −4.0 V; (b) the applied voltage was swept from 0 to +4.0 V. The electrode contact area was 0.5 × 0.5 mm^2.

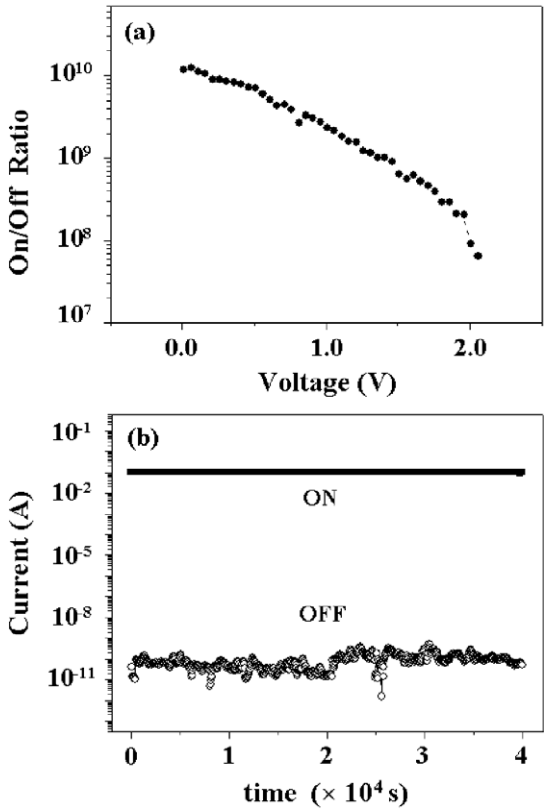

Figure 3. (a) ON/OFF current ratios for the Au/6F-2TPA PI (74 nm thick)/Al device measured during the voltage sweeps as a function of the applied voltage. (b) Retention times of the ON and OFF states of the Au/6F-2TPA PI (74 nm thick)/Al device, as probed with a reading voltage of +1.0 V.

electrode, i.e. the PI films coated onto the metal electrodes have smooth surfaces. In addition, the highest occupied molecular orbital (HOMO) and the lowest unoccupied molecular orbital (LUMO) energy levels of the 6F-2TPA PI were determined. The HOMO and LUMO levels of the 6F-2TPA PI were found to be −5.10 eV and −1.88 eV, respectively, by using ultraviolet–visible spectroscopy and cyclic voltammetry.

Figure 2 shows typical current–voltage (I–V) characteristics of Au/6F-2TPA PI (74 nm thick)/Al sandwich devices (figure 1(b)), which were measured with a compliance current set of 0.1 A. As can be seen in figure 2(a), the as-fabricated 6F-2TPA PI film initially exhibits a low-conductivity state (the OFF state). During the negative voltage sweep up to approx. −1.8 V, the device is not switched to a high-conductivity state (the ON state). However, when the applied voltage was increased further, a sharp increase in the current was observed, indicating that the device undergoes an electrical transition from the OFF state to the ON state. In a memory device, this OFF-to-ON-state transition can function as a 'writing' process. Once the device has reached its ON state, it remains there, even after the power is turned off, and furthermore cannot be returned to the OFF state by applying an opposite bias or even by applying negative and positive voltages with various compliance current sets. Similar electrically bistable switching characteristics were observed when a positive bias was applied. The electrical transition voltage was found to be 2.1 V (figure 2(b)). Overall, this device exhibits excellent WORM memory behavior.

Figure 3(a) shows the ratio of the OFF-to-ON-state current for the 74 nm thick 6F-2TPA PI devices as a function of the applied voltage during the positive sweep, which was measured with a probing (i.e. reading) voltage of 1.0 V. The ON/OFF current ratio is 10^7–10^{10} in the voltage range 0–4.0 V. Figure 3(b) shows representative results of the retention tests carried out on the 74 nm thick 6F-2TPA PI devices under a positive bias and ambient conditions. Similar retention test results were obtained under a negative bias (data not shown). Once the device is switched to the ON state by applying a positive voltage pulse (1.0 V), the ON state is retained without any degradation for more than 10 h.

To understand the observed memory characteristics, we considered the HOMO and LUMO levels of the 6F-2TPA PI and the work functions (Φ) of the Al top and Au bottom electrodes: Φ is −5.1 eV for Au and −4.2 eV for Al. In the Au/6F-2TPA PI/Al devices, the energy barrier between the work function Φ of the Au bottom electrode and the HOMO level of the active 6F-2TPA PI layer is zero, which is much smaller than that (2.32 eV) between the LUMO level of the active 6F-2TPA PI layer and the work function Φ of the Al top electrode. Thus hole injection from the Au bottom electrode into the HOMO level of the 6F-2TPA PI layer is much more favorable than electron injection from the Al top electrode into the LUMO level of the 6F-2TPA PI layer, and hole injection dominates the conduction process in the devices. Furthermore,

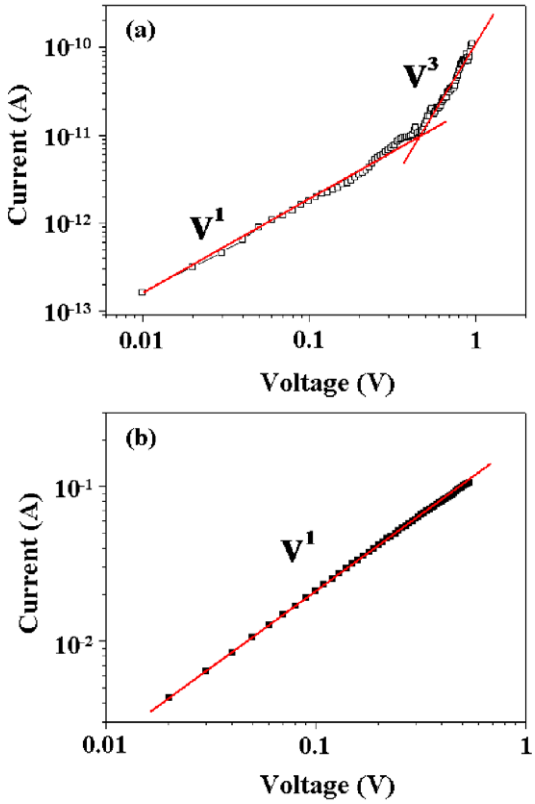

Figure 4. Experimental and fitted I–V curves for the Au/6F-2TPA PI (74 nm thick)/Al device: (a) OFF state with a combination of the ohmic model and the space-charge-limited model and (b) ON state with the ohmic model.

current flow under a negative bias is more favorable than that under a positive bias.

The measured I–V characteristics of the devices were further analyzed in detail with various conduction models in order to understand their electrical switching characteristics [20–24]. The trap-limited space-charge-limited conduction (SCLC) model was found to satisfactorily fit the I–V data for the OFF state. As shown in figure 4(a), the logarithmic plot of the I–V data for the OFF state contains two linear regions for $<$0.43 V and $\geqslant$0.43 V, with slopes of 1.0 and 3.0, respectively. These results indicate that a trap-limited SCLC mechanism is dominant when the device is in the OFF state. The ohmic contact model was found to satisfactorily fit the I–V data for the ON state. As can be seen in figure 4(b), the logarithmic plot of the I–V data for the ON state contains a linear region with a slope of 1.0, indicating that ohmic conduction is dominant when the device is in the ON state. Moreover, the current level of our devices in the ON state was found not to be dependent on the device cell size, which is indicative of heterogeneously local filament formation.

The above results suggest that the excellent WORM memory behavior of the 6F-2TPA PI films is governed by trap-limited SCLC and local filament formation. The trapping sites might arise because of the chemical composition of the 6F-2TPA PI chain, which contains a 2TPA unit, a trifluoromethyl group and two imide rings per repeat unit of the backbone. In the PI chain, the 2TPA units are electron donors and thus can act as nucleophilic sites, whereas the trifluoromethyl groups and the imide rings are electron acceptors and can act as electrophilic sites. Thus all these groups could act as charge-trapping sites, depending on their associations. As discussed above, for the 6F-2TPA PI the energy barrier for hole injection is lower than that for electron injection, so the conduction process in the 6F-2TPA PI device is dominated by hole injection. Thus the 2TPA units might act as hole-trapping sites, which would explain the observed WORM memory behavior of the 6F-2TPA PI-based devices. The 2TPA units in the 6F-2TPA PI film are enriched with holes when a bias is applied. At the same time, the trifluoromethyl groups and imide rings in the PI film are enriched with electrons. When the applied bias reaches the threshold voltage, the trapped charges are able to move through the trapped sites by means of a hopping process (i.e. through filament formation), which results in current flow between the bottom and top electrodes.

Taking into consideration the above excellent memory characteristics, we fabricated devices with 6F-2TPA PI films of various thicknesses (15, 34, 100 and 150 nm) and investigated their memory performance. We found that the 15 nm thick 6F-2TPA PI films always exhibit high conductivity (i.e. the ON state) in positive and negative voltage sweeps for a compliance current window of 1.0×10^{-4}–1.0×10^{-1} A, which are the limits of the semiconductor analyzer used in our study. Representative I–V results for the 15 nm thick films are shown in figure 5. As observed for the 15 nm thick films, the 34 nm thick films exhibit high conductivity (i.e. the ON state) in negative voltage sweeps (figure 5(a)), with no electrical switching behavior. However, as observed for the 74 nm thick 6F-2TPA PI films, the 34 nm thick films do exhibit WORM memory characteristics in positive voltage sweeps (figure 5(b)). The switching-on voltage was found to be 1.1 V during the positive voltage sweep. This switching threshold voltage is lower than that (2.1 V) of the 74 nm thick 6F-2TPA PI films. These results suggest that in these devices thinner 6F-2TPA PI films have lower switching threshold voltages. In contrast, the 100 nm thick 6F-2TPA PI films exhibit switching characteristics during the negative voltage sweeps (figure 5(a)) but always exhibit low conductivity (i.e. the OFF state) during positive voltage sweeps (figure 5(b)). Furthermore, the 150 nm thick 6F-2TPA PI films only exhibit low conductivity in positive and negative sweeps, with no electrical switching behavior (figure 5).

In particular, the electrical switching behavior observed during the negative voltage sweeps of the 100 nm thick films was found to be quite different from the WORM memory characteristics observed for the 34 and 74 nm thick films. Figure 6 shows typical I–V characteristics of the 100 nm thick films with Au top and Al bottom electrodes, which were measured in a dual sweep mode with negative bias (0 V $\rightarrow$ -4.0 V $\rightarrow$ 0 V). Initially, the device is in the OFF state. In this OFF state, the current level is quite low (of the order of 10^{-14}–10^{-9} A). In the first dual sweep (see the first sweep in figure 6), there is an abrupt increase in the current (from 10^{-11} to 10^{-1} A) at -3.3 V (which corresponds to the switching threshold voltage), which indicates that the film undergoes

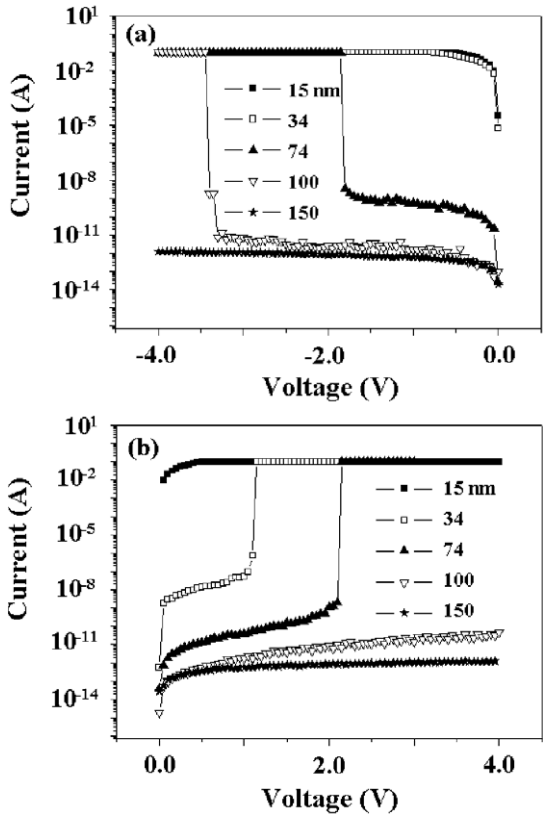

Figure 5. I–V curves for the devices fabricated with 6F-2TPA PI films of various thicknesses (15–150 nm) and Au top and Al bottom electrodes: (a) the applied voltage was swept from 0 to −4.0 V; (b) the applied voltage was swept from 0 to +4.0 V. The electrode contact area was 0.5 × 0.5 mm^2.

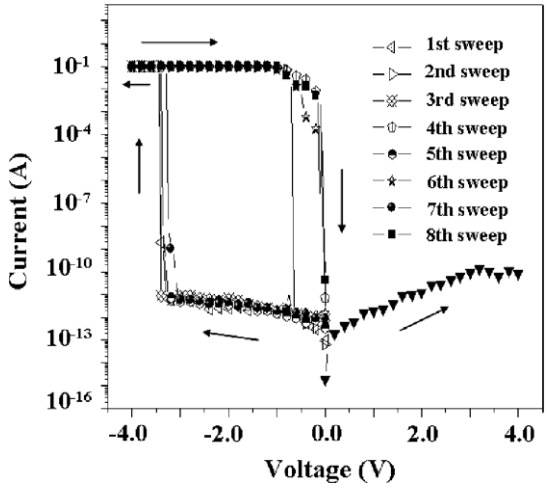

Figure 6. I–V curves for the Au/6F-2TPA PI (100 nm thick)/Al devices. The I–V measurements were performed in a dual sweep mode with negative bias (0 V → −4.0 V → 0 V). Positive voltage sweep measurements were also carried out. The electrode contact area was 0.5 × 0.5 mm^2.

an electrical transition from the OFF state to the ON state. This electrical transition can serve as the 'writing' process in a memory device. When a reverse voltage sweep is applied, the film is reset to the initial low-conductivity state (i.e. the OFF state), which can serve as the 'erasing' process in the memory device. The erased state can be again written to the stored state when the switching threshold voltage is applied (see the second sweep in figure 6), indicating that the memory device is rewritable. The third sweep was carried out after turning off the power for about 2–5 s. It was found that the ON state had relaxed to the steady OFF state. However, the film can be further programed to the ON state. The short retention time of the ON state indicates that the memory device is volatile. The above processes can be repeated many times for every cell (figure 6). Overall, the 100 nm thick films exhibit interesting and unique dynamic random access memory (DRAM) characteristics during negative voltage sweeps.

The above I–V results confirm that the 6F-2TPA PI-based devices exhibit excellent WORM and DRAM memory characteristics as well as polarity-dependent turn-on behaviors when the thicknesses of the active polymer layers in the devices are varied.

These extreme thickness-dependent I–V results can be understood by considering the HOMO and LUMO levels and thicknesses of the 6F-2TPA PI film, the work functions of the top and bottom electrodes, and the switching mechanism discussed above. The 15 nm thick films are too thin and so allow high conductance ohmic current flow (i.e. short circuit current flow) under both positive and negative bias, which overrides the energy barrier levels between the film and the electrodes. The properties of the 34 nm thick films are somewhat different: during a negative voltage sweep short circuit current flow is still possible due to the zero energy barrier between the Au bottom electrode and the film. However, such short circuit current flow is prevented during the positive voltage sweep by the relatively high energy barrier (2.32 eV) between the film and the Al bottom electrode, which results in WORM memory characteristics based on the trap-limited SCLC and local filament formation.

In contrast, the 74 and 100 nm thick films appear to be sufficiently thick to completely prevent short circuit current flow under both positive and negative biases, even though the energy barrier between the Au top electrode and the film is zero, because 6F-2TPA PI is more like an insulator than a conductor; the 6F-2TPA PI films' conductivity was measured to range between 1.0×10^{-13}–1.0×10^{-14} S cm^{-1}. The above results indicate that the 74 nm thick films are likely to exhibit WORM memory characteristics during both the positive and negative voltage sweeps that are governed by trap-limited SCLC and stable local filament formation. However, the 100 nm thick films are slightly too thick to exhibit WORM memory behavior. Moreover, local filament formation during the positive voltage sweep appears to be completely prevented because of the relatively high energy barrier between the film and the electrode, which means that there is no electrical switching behavior. On the other hand, from the zero energy barrier between the Au top electrode and the film it is expected that electrical switching behavior occurs during the negative voltage sweep. However, these films are too thick to exhibit stable local filament formation, i.e., only unstable local filaments form in the films. Thus, the 100 nm thick films exhibit only DRAM memory behavior

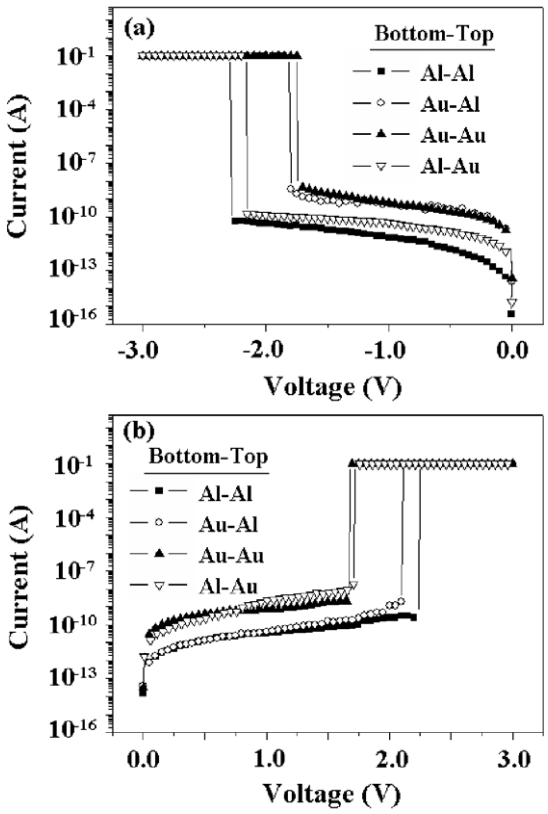

Figure 7. *I–V* curves for the 74 nm thick 6F-2TPA PI-based devices fabricated with various pairs of top and bottom electrodes: (a) the applied voltage was swept from 0 to −3.0 V; (b) the applied voltage was swept from 0 to +3.0 V. The electrode contact area was 0.5×0.5 mm^2.

rather than WORM memory behavior. The 150 nm thick films are too thick to allow local filament formation during either the positive or negative voltage sweeps, and so exhibit no electrical switching behavior at all.

In addition, we fabricated devices with 74 nm thick 6F-2TPA PI films and various top–bottom electrode pairs (Al–Al, Au–Au and Al–Au) and investigated their electrical performance. The measured *I–V* characteristics are presented in figure 7. As can be seen in this figure, all the devices exhibit WORM memory behavior, regardless of which top–bottom electrode pair was used or the voltage sweep direction. Only the switching-on voltage and the ON state current level vary with the top–bottom electrode pair and the voltage sweep direction; these variations are attributed to the relationships between the work functions of the electrodes and the HOMO and LUMO levels of the 6F-2TPA PI.

4. Conclusion

We have fabricated electrically programmable memory devices with thermally and dimensionally stable 6F-2TPA PI films and investigated their switching characteristics and reliability. The 6F-2TPA PI films exhibit versatile memory characteristics that depend on the film thickness. All the PI films are initially present in the OFF state. The PI films with thicknesses in the range 34–74 nm exhibit excellent WORM (i.e. fuse-type) memory characteristics with and without polarity depending on the thickness. The WORM memory devices are electrically stable, even in air ambient, for a very long time. The devices' ON/OFF current ratio is high, up to 10^{10}. Therefore, these WORM memory devices can provide an efficient, low-cost means of permanent data storage. On the other hand, the 100 nm thick PI films exhibit excellent DRAM memory characteristics with polarity. The ON/OFF current ratio of the DRAM devices is as high as 10^{11}. These properties open up the possibility of the low-cost mass production of high density and very stable digital nonvolatile WORM and volatile DRAM memory devices.

Acknowledgments

This study was supported by the Korea Science and Engineering Foundation (National Research Laboratory for Polymer Synthesis and Physics and Center for Electro-Photo Behaviors in Advanced Molecular Systems) and by the Ministry of Education, Science and Technology (MEST) (BK21 Program). This work was also supported by the National Science Council of the Republic of China.

References

[1] Donhauser Z J *et al* 2001 *Science* **29** 2303
[2] Tu C-H, Lai Y-S and Kwong D-L 2006 *Appl. Phys. Lett.* **89** 062105
[3] Kolosov D, English D S, Bulovic V, Barbara P F, Forrest S R and Thompson M E 2001 *J. Appl. Phys.* **90** 3242
[4] Yang Y, Ouyang J, Ma L, Tseng R J-H and Chu C-W 2006 *Adv. Funct. Mater.* **16** 1001
[5] Scott J C and Bozano L D 2007 *Adv. Mater.* **19** 1452
[6] Ma D, Aguiar M, Freire J A and Hümmelgen I A 2006 *Adv. Mater.* **12** 1063
[7] Henisch H K, Meyers J A, Callarotti R C and Schmidt P E 1978 *Thin Solid Films* **51** 265
[8] Ling Q, Song Y, Ding S J, Zhu C, Chan D S H, Kwong D-L, Kang E-T and Neoh K-G 2005 *Adv. Mater.* **17** 455
[9] Smits J H A, Meskers S C J, Janssen R A J, Marsman A W and de Leeuw D M 2005 *Adv. Mater.* **17** 1169
[10] Baek S, Lee D, Kim J, Hong S-H, Kim O and Ree M 2007 *Adv. Funct. Mater.* **17** 2637
[11] Lee D, Baek S, Ree M and Kim O 2008 *IEEE Electron Device Lett.* **29** 694
[12] Kim J, Cho S, Choi S, Baek S, Lee D, Kim O, Park S-M and Ree M 2007 *Langmuir* **23** 9024
[13] Hong S-H, Kim O, Choi S and Ree M 2007 *Appl. Phys. Lett.* **91** 093517
[14] Choi S, Hong S-H, Cho S H, Park S, Park S-M, Kim O and Ree M 2008 *Adv. Mater.* **20** 1766
[15] Hahm S G, Choi S, Hong S-H, Lee T J, Park S, Kim D M, Kwon W-S, Kim K, Kim O and Ree M 2008 *Adv. Funct. Mater.* **18** 3276
[16] Kim Y, Ree M, Chang T, Ha C S, Nunes T L and Lin J S 1995 *J. Polym. Sci.* B **33** 2075
Kim S I, Pyo S M and Ree M 1997 *Macromolecules* **30** 7890
Ree M, Kim K, Woo S H and Chang H 1997 *J. Appl. Phys.* **81** 698
Pyo S M, Kim S I, Shin T J, Ree M, Park K H and Kang J S 1998 *Macromolecules* **31** 4777
Shin T J and Ree M 2005 *Langmuir* **21** 6081
Ree M 2006 *Macromol. Res.* **14** 1
Shin T J and Ree M 2007 *J. Phys. Chem.* B **111** 13894

[17] Geary J M, Goodby J W, Kmetz A R and Patel J S 1987 *J. Appl. Phys.* **62** 4100
Toney M F, Russell T P, Logan J A, Kikuchi H, Sands J M and Kumar S K 1995 *Nature* **374** 709
Lee K-W, Paek S-H, Lien A, Durning C and Fukuro H 1996 *Macromolecules* **29** 8894
Kim S I, Ree M, Shin T J and Jung J C 1999 *J. Polym. Sci.* A **37** 2909
Ge J J *et al* 2001 *J. Am. Chem. Soc.* **123** 5768
Chae B, Kim S B, Lee S W, Kim S I, Choi W, Lee B, Ree M, Lee K H and Jung J C 2002 *Macromolecules* **35** 10119
Chae B, Lee S W, Lee B, Choi W, Kim S B, Jung Y M, Jung J C, Lee K H and Ree M 2003 *J. Phys. Chem.* B **107** 11911
Lee S W, Chae B, Kim H C, Lee B, Choi W, Kim S B, Chang T and Ree M 2003 *Langmuir* **19** 8735
Chae B, Lee S W, Lee B, Choi W, Kim S B, Jung Y M, Jung J C, Lee K H and Ree M 2003 *Langmuir* **19** 9459
Lee S W, Chae B, Lee B, Choi W, Kim S B, Kim S I, Park S-M, Jung J C, Lee K H and Ree M 2003 *Chem. Mater.* **15** 3105
Lee S W *et al* 2005 *Macromolecules* **38** 4331
Hahm S G, Lee T J, Chang T, Jung J C, Zin W-C and Ree M 2006 *Macromolecules* **39** 5385
Hahm S G, Lee S W, Suh J, Chae B, Kim S B, Lee S J, Lee K H, Jung J C and Ree M 2006 *High Preform. Polym.* **18** 549
[18] Lee S W, Kim S I, Lee B, Choi W, Chae B, Kim S B and Ree M 2003 *Macromolecules* **36** 6527
Lee S W, Kim S I, Lee B, Kim H C, Chang T and Ree M 2003 *Langmuir* **19** 10381
Hahm S G, Lee T J and Ree M 2007 *Adv. Funct. Mater.* **17** 1359
Hahm S G, Lee S W, Lee T J, Cho S A, Chae B, Jung Y M, Kim S B and Ree M 2008 *J. Phys. Chem.* B **112** 4900
[19] Cheng S-H, Hsiao S-H, Su T-H and Liou G-S 2005 *Macromolecules* **38** 307
[20] Campell A J, Bradley D D C and Lidzey D G 1997 *J. Appl. Phys.* **82** 6326
[21] Jensen K L 2003 *J. Vac. Sci. Technol.* B **21** 1528
[22] Mark P and Helfrich W 1962 *J. Appl. Phys.* **33** 205
[23] Frenkel J 1938 *Phys. Rev.* **54** 647
[24] Laurent C, Kay E and Souag N 1988 *J. Appl. Phys.* **64** 336